



2 **A splitting of collinear libration points in circular restricted**
3 **three-body problem by an artificial electrostatic field**

4 Vladimir S. Aslanov

5 Received: 24 December 2020 / Accepted: 16 January 2021
6 © The Author(s), under exclusive licence to Springer Nature B.V. part of Springer Nature 2021

7 **Abstract** This paper focuses on the study of a new
8 type of a planar, circular restricted three-body problem
9 with an attractive artificial electrostatic field (E-field)
10 at collinear libration points. For instance, this attrac-
11 tive field can be generated by an orbiting spacecraft
12 located at the Mars-Phobos L1 libration point and an
13 electrostatic capsule launched from Phobos. The
14 feasibility of the proposed retrieval system is dis-
15 cussed from the aspect of local space weather Debye
16 length. The attractive E-field splits the collinear
17 libration point into two new collinear points, and the
18 greater the E-field potential and the Debye length the
19 greater the distance between the new libration points
20 and the “old” original libration point. The new
21 equilibrium positions caused by the action of the
22 E-field have been found, and an instability of these
23 new libration points has been proven. A new Jacobi
24 integral in analytical form is obtained and equations of
25 motion are derived for the restricted problem of three
26 bodies taking into account the E-field. A numerical
27 simulation shows the impact of the E-field potential on
28 capsule capture in the small vicinity of the Mars-
29 Phobos L1 libration point. This work expands the
30 classic three-body problem filling with new content.
31 The obtained results can be applied, for example, to

study an opportunity of delivering the Phobos samples 32
using Coulomb interaction of bodies in space. 33

Keywords Libration points · Electrostatic field · 34
Stability and instability · Exact solutions · Jacobi 35
integral 36

1 Introduction 37

The planar circular restricted three-body problem is a 38
classic celestial mechanics issue. Its study made a 39
great contribution to the theory of space dynamics and 40
celestial mechanics. The restricted three-body prob- 41
lem is the basis for solving many applied tasks in 42
astronautics, in particular, for calculating interplane- 43
tary flights and launching spacecraft and satellites. 44
This problem and its various aspects received great 45
attention from the scientific community. A detailed 46
analysis of major studies on this topic can be found in 47
the Szebehely’s textbook [1]. The book discusses the 48
regularization of the motion equations, manifold of the 49
states of motion, equilibrium positions, motion near 50
these positions, application of Hamiltonian dynamics 51
methods to the restricted problem, its periodic orbits 52
and quantitative aspects. A detailed numerical analysis 53
of three-dimensional periodic halo orbits near colli- 54
near libration points in the restricted three-body 55
problem was performed by Howell [2]. Analytical 56

A1 V. S. Aslanov (✉)
A2 Samara National Research University, 34, Moscovskoe
A3 shosse, Samara, Russia 443086
A4 e-mail: aslanov_vs@mail.ru
A5 URL: http://aslanov.ssau.ru/

57 solutions for Lissajous and halo orbits near collinear
 58 points L_1, L_2 were obtained by Luo et al. in [3] using
 59 normalization method. These results were compared
 60 with the solutions obtained by Lindstedt–Poincaré
 61 method. Numerical analysis of the planar circular
 62 restricted three-body problem phase space and orbits
 63 classification into three groups (bounded, escape and
 64 collisional) were performed by Zotos [4]. Halo,
 65 Lyapunov and vertical orbits for elliptic restricted
 66 three-body problem were studied based on resonant
 67 motions in the circular problem by Ferrari and
 68 Lavagna [5]. Woo and Misra [6] investigated the
 69 spacecraft motion in the vicinity of a binary asteroid
 70 system as the circular restricted case. The asteroids
 71 were considered as rigid bodies. Addition equilibrium
 72 points were found numerically for some special cases.
 73 Biggs and Negri [7] considered solar sail spacecraft
 74 controlled motion within the circular restricted three-
 75 body problem. The spacecraft moves in the gravita-
 76 tional field of the Earth and the Moon, taking into
 77 account the perturbation introduced by the solar
 78 pressure on the sail. Alessi and Sánchez [8] presented
 79 a semi-analytical approach, which is based on a
 80 perturbation procedure, for study the three-dimen-
 81 sional motion of a negligible mass body in the circular
 82 restricted three-body problem. At this point, it should
 83 be emphasized that the above references are not an
 84 exhaustive analysis of the literature on the considered
 85 topic, which is very broad and includes a huge number
 86 of works, but they give some insight into this problem.
 87 New engineering ideas require solutions of new
 88 fundamental problems. For example, in recent years,
 89 Martian sample return missions were actively dis-
 90 cussed by scientists [9]. The missions assume that a
 91 sample capsule is launched from Mars surface using a
 92 Mars Ascent Vehicle after samples are collected by a
 93 rover [10]. As a solution to a deep-space docking
 94 challenge, the ability to use electrostatic force to
 95 capture the container was discussed in [9]. The idea of
 96 an electrostatic capture of the capsule can be used also
 97 in the case when an orbital spacecraft (orbiter) is
 98 located, in contrast to [9], at one of the collinear
 99 libration points.

100 If we talk about Mars, then it can be point L_3 , and if
 101 about Mars’s moon, Phobos, then points L_1 and L_2 are
 102 more suitable. The Phobos exploration is of indepen-
 103 dent importance. Phobos is a small, irregularly shaped
 104 moon ($\sim 26 \times 22.8 \times 18.1$ km) that orbits Mars
 105 every 7 h and 39 min. The orbit is synchronous to its

106 rotation so that its long axis is always directed toward
 107 Mars. The Mars-Phobos L_1 libration point is unusually
 108 close to Phobos’ surface (~ 3.4 km), and it make the
 109 capsule delivery mission to a Phobos Sample Return
 110 orbiter technically feasible if the orbiter hovered in the
 111 Mars-Phobos L_1 point. Several theoretical questions
 112 have to be answered in order to investigate a
 113 possibility of using the attractive artificial E-field at
 114 the collinear libration points L_1, L_2 and L_3 , for
 115 example, the Phobos sample capsule delivery mission.

116 The answers to these questions are covered in this
 117 article. This study focuses on equations and analytical
 118 formulas describing the new planar circular restricted
 119 three-body problem with the additional E-field. The
 120 goal is to understand the body’s behavior in the E-field
 121 and the two gravitational fields caused by the main
 122 bodies near the collinear libration points. Note that
 123 when considering the E-field, the Debye length λ_D
 124 must be taken into account. The Debye length is an
 125 important parameter because the E-field rapidly
 126 decreases beyond this length by the Debye shielding
 127 effect. The motion equations are written in a rotating
 128 Cartesian coordinate system, which is converted to a
 129 canonical dimensionless form. We show the splitting
 130 of the “old” collinear libration points L_1, L_2, L_3 , and
 131 find new paired equilibrium positions ($L_{1+}, L_{1-}; L_{2+},$
 132 $L_{2-}; L_{3+}, L_{3-}$) in the vicinity of the “old” points, and
 133 also prove the instability of these new equilibrium
 134 positions. Next, a new Jacobi integral is obtained in
 135 analytical form for the circular restricted three-body
 136 problem taking into account the E-field. And finally,
 137 using numerical modeling, we show the effect of the
 138 E-field potential on the capture of the electrostatic
 139 capsule (E-capsule) in the small vicinity of the Mars-
 140 Phobos L_1 libration point.

2 Equations of motion and Jacobi integral 141

142 In this section, we derive the planar motion equations
 143 of a body in two gravitational and one attractive E-
 144 field. The center of E-field is located at a single
 145 collinear libration point. These points are called the
 146 “old” collinear libration points because, as can be
 147 assumed (this will be proved below), due to the action
 148 of the E-field, the “old” unstable point splits into two
 149 new unstable equilibrium points. The action of the E-
 150 fields is limited to the Debye length within tens of
 151 meters. In addition, the motion of a body is studied

152 only in a small vicinity of “old” points comparable to
 153 Debye length, beyond which the problem degenerates
 154 into the classic three-body problem. Therefore, we talk
 155 about two gravity fields and one attractive E-field, and
 156 the motion equations are written for the vicinity of
 157 each point: L_1, L_2, L_3 . The equations of motion are
 158 derived using classical terminology of the three-body
 159 problem presented in book by Schaub and Junkins
 160 [11]. This will facilitate understanding of the pre-
 161 sented material. Below this section is organized as
 162 follows. Firstly, the conventional assumptions for the
 163 circular restricted three-body problem are described.
 164 Next, the expression for Coulomb force acting on the
 165 charged body in the E-field is given. Then, the
 166 equations of the body motion are derived in canonical
 167 form. Finally, the non-dimensional potential function
 168 and the Jacobi integral are found.

169 The considered mechanical system consists of three
 170 bodies M_1, M_2 and M (Fig. 1). It is assumed that the
 171 mass of the body M is many times less than the mass of
 172 the bodies M_1 and M_2 . Therefore, the body M has
 173 negligible effect on the other bodies. It is also
 174 supposed that the bodies M_1 and M_2 move in circular
 175 orbits around their mutual center of mass. Before
 176 proceeding with the construction of the relative
 177 motion equations, the electrostatic force is introduced.
 178 The orbiter is assumed to be located at one of the
 179 collinear libration points of $M_1 - M_2$ bodies system and
 180 to have an electrostatic charge. The mass of the orbiter
 181 is not taken into account. The charged electrostatic
 182 capsule (E-capsule) is affected by an electrostatic
 183 force when moving in the vicinity of the orbiter. The
 184 capsule performance is dependent on this force. It is
 185 assumed that the capsule and the orbiter are perfectly

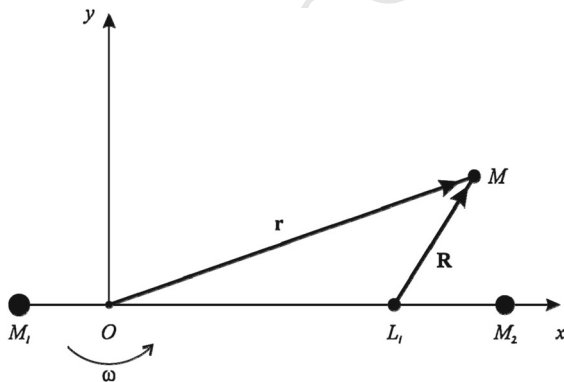


Fig.1 The Local-Vertical-Local-Horizontal frame Oxy

conducting spheres. The electrostatic force between
 the capsule and orbiter is defined by the equation

$$F = k_C \frac{q_o q}{R^2} \tag{1}$$

where $k_C = 8.99 \cdot 10^9 Nm^2/C^2$ is the Coulomb constant, q_o is the charge on the orbiter, q is the charge on the capsule, R is the distance between the capsule and orbiter. Note that this force may be either attractive or repulsive depending on the polarity of the potentials of the E-capsule and orbiter. Consider only the attracting configuration ($q_o q < 0$) in this paper.

Let us first introduce into consideration three vectors in the Local-Vertical-Local-Horizontal frame Oxy : the position vector of the body M (Fig. 1)

$$\mathbf{r} = (r_x, r_y) \tag{2}$$

the vector $\mathbf{a} = (a, 0)$ determines the position of the collinear libration points L_1, L_2 and L_3 in the frame Oxy

$$a = (a_1, a_2, a_3), \quad a_i = |\overline{OL_i}|, \quad i = 1, 2, 3 \tag{3}$$

and, the position vector of the body M with respect to the collinear libration point (Fig. 1)

$$\mathbf{R} = \mathbf{r} - \mathbf{a} = (X = r_x - a, Y = r_y) \tag{4}$$

Then, the vector of the Coulomb force (1) is written as

$$\mathbf{F} = kF \frac{\mathbf{R}}{R} = k \frac{k_C q_o q}{R^3} \mathbf{R}, \quad (q_o q < 0) \tag{5}$$

Note that the Coulomb force affects the body M , if this body is within the Debye length of a collinear libration point, i.e., within 10 s meters

$$k = \begin{cases} 1, & \sqrt{(r_x - a)^2 + r_y^2} \leq \lambda_D \\ 0, & \sqrt{(r_x - a)^2 + r_y^2} > \lambda_D \end{cases} \tag{6}$$

Now, taking into account the Coulomb force (5), the equations of the E-capsule planar motion can be written the frame Oxy [11]

$$\ddot{r}_x = \frac{\partial W}{\partial r_x} + \omega^2 r_x + 2n\dot{r}_y + k \frac{k_C q_o q}{m} \frac{(r_x - a)}{R^3} \tag{7}$$

$$\ddot{r}_y = \frac{\partial W}{\partial r_y} + \omega^2 r_y - 2n\dot{r}_x + k \frac{k_C q_o q}{m} \frac{r_y}{R^3} \tag{8}$$

$$W(r_x, r_y) = G \left(\frac{m_1}{\sqrt{(r_x + d\mu)^2 + r_y^2}} + \frac{m_2}{\sqrt{(r_x - d(1-\mu))^2 + r_y^2}} \right) \tag{9}$$

222 where $\mu = \frac{m_2}{m_1+m_2}$; ω is a constant angular velocity
 223 magnitude of the M_1 - M_2 system; d is the distance
 224 between M_1 and M_2 ; m, m_1 and m_2 are masses of the
 225 bodies M, M_1 and M_2 , respectively.

226 The motion equations (7) and (8) can be written in a
 227 convenient non-dimensional form. To do so, we
 228 introduce the non-dimensional time variable t as

$$\tau = \omega t \tag{10}$$

230 Time derivatives with respect to this new time
 231 variable are denoted as

$$(\cdot)' = \frac{d}{d\tau}(\cdot) \tag{11}$$

233 Any scalar distances are non-dimensionalized by
 234 dividing them with the constant relative between M_1
 235 and M_2 as

$$x = \frac{r_x}{d}, y = \frac{r_y}{d} \tag{12}$$

237 Using the variables substitutions (10) and (12), we
 238 now are able to rewrite Eqs. (7) and (8) into the
 239 following non-dimensional form:

$$x'' - 2y' = \frac{\partial U}{\partial x} \tag{13}$$

$$241 \quad y'' + 2x' = \frac{\partial U}{\partial y} \tag{14}$$

243 where $\alpha = \frac{a}{d} < 1$. The corresponding non-dimensional
 244 potential function $U(x, y)$ is given by the expression

$$U(x, y) = \frac{1}{2}(x^2 + y^2) + \frac{1-\mu}{\sqrt{(\mu+x)^2 + y^2}} + \frac{\mu}{\sqrt{(-1+\mu+x)^2 + y^2}} - k \frac{\Phi}{\sqrt{(x-\alpha)^2 + y^2}} \tag{15}$$

246 where

$$\Phi = \frac{kcqoq}{md^3\omega^2} < 0 \tag{16}$$

Due to the definition of the mass ratio μ the non-
 dimensional coordinates of M_1 and M_2 are written as.

$$x_1 = -\mu, \quad x_2 = 1 - \mu \tag{17}$$

This expression is simplified by entering a non-
 dimensional relative distance ρ_i is defined as

$$\rho_i = \sqrt{(x - x_i)^2 + y^2}, \quad \rho = \sqrt{(x - \alpha)^2 + y^2} \tag{18}$$

Then, the corresponding non-dimensional potential
 function (15) is given by the expression

$$U(x, y) = \frac{1}{2}(x^2 + y^2) + \frac{1-\mu}{\rho_1} + \frac{\mu}{\rho_2} - k \frac{\Phi}{R} \tag{19}$$

Following similar steps as were done with the
 classic restricted three-body problem [11], with the E-
 field the non-dimensional Jacobi integral takes on the
 form

$$J(x, y) = (x^2 + y^2) + \frac{2(1-\mu)}{\sqrt{(\mu+x)^2 + y^2}} + \frac{\mu}{\sqrt{(-1+\mu+x)^2 + y^2}} - 2k \frac{\Phi}{\sqrt{(x-\alpha)^2 + y^2}} - (x^2 + y^2) \tag{20}$$

For the dimensional equations of motion (13) and
 (14) the non-dimensional Jacobi integral is written as

$$J(x, y) = (x^2 + y^2) + \frac{2(1-\mu)}{\rho_1} + \frac{2\mu}{\rho_2} - 2k \frac{\Phi}{\rho} - (x^2 + y^2) \tag{21}$$

3 New Lagrange collinear libration points

Setting the relative velocities and accelerations in
 Eqs. (13) and (14) equal to zero, we find conditions
 that are satisfied by the stationary points of the circular
 restricted three-body problem with the E-field. Obvi-
 ously, the new stationary points can be located only
 within the Debye length of the “old” collinear
 libration points L_i ($i = 1, 2, 3$), i.e., within tens of
 meters. Outside this boundary, this task degenerates
 into the classic circular restricted three-body problem
 when, $k = 0$ according to Eqs. (6), (13) and (14).

Author Proof

277 Therefore, we will look for new libration points only
 278 inside the Debye sphere is defined as

$$\sqrt{(r_x - a)^2 + r_y^2} \leq \lambda_D \tag{22}$$

280 or, taking into account (12)

$$\sqrt{(x - \alpha)^2 + y^2} \leq \frac{\lambda_D}{d} = l_D \tag{23}$$

282 To solve for the scalar coordinate x for the collinear
 283 libration points, Eq. (13) is set equal to zero for
 284 $y' = y = 0$, simplify to following [11]

$$0 = x - \frac{\mu(-1 + \mu + x)}{(-1 + \mu + x)^3} - \frac{(1 - \mu)(\mu + x)}{(\mu + x)^3} + k \frac{\Phi(x - \alpha)}{(x - \alpha)^3} \tag{24}$$

286 Let's rewrite Eq. (24) with regard to (17) as

$$0 = x - \frac{\mu(x - x_2)}{(x - x_2)^3} - \frac{(1 - \mu)(x - x_1)}{(x - x_1)^3} + k \frac{\Phi(x - \alpha)}{(x - \alpha)^3} \tag{25}$$

288 Using the fact that the new libration points gener-
 289 ated by the E-field must be located within the Debye
 290 sphere (23), we begin with the vicinity of the point L_{1-}
 291 and find from Eq. (25) implicit conditions for the L_{1-}
 292 and L_{1+} position coordinates in terms of the mass ratio
 293 μ :

$$L_{1-} : 0 = x - \frac{1 - \mu}{(\mu + x)^2} + \frac{\mu}{(x - 1 + \mu)^2} - \frac{\Phi}{(x - \alpha)^2} \tag{26}$$

$$L_{1+} : 0 = x - \frac{1 - \mu}{(\mu + x)^2} + \frac{\mu}{(x - 1 + \mu)^2} + \frac{\Phi}{(x - \alpha)^2} \tag{27}$$

297 The last terms differentiate these equations from
 298 Eq. (10.93) in [11] and show the splitting of the point
 299 L_1 into two new unstable collinear points L_{1-} and L_{1+} .
 300 Now consistently, in a similar way, we write down the
 301 implicit conditions for the collinear libration points in
 302 the vicinity of the "old" libration points L_2 and L_3 :

$$L_{2-} : 0 = x - \frac{1 - \mu}{(\mu + x)^2} - \frac{\mu}{(x - 1 + \mu)^2} - \frac{\Phi}{(x - \alpha)^2} \tag{28}$$

304

$$L_{2+} : 0 = x - \frac{1 - \mu}{(\mu + x)^2} - \frac{\mu}{(x - 1 + \mu)^2} + \frac{\Phi}{(x - \alpha)^2} \tag{29}$$

and

$$L_{3-} : 0 = x + \frac{1 - \mu}{(\mu + x)^2} + \frac{\mu}{(x - 1 + \mu)^2} + \frac{\Phi}{(x - \alpha)^2} \tag{30}$$

$$L_{3+} : 0 = x + \frac{1 - \mu}{(\mu + x)^2} + \frac{\mu}{(x - 1 + \mu)^2} - \frac{\Phi}{(x - \alpha)^2} \tag{31}$$

The order of the location of the new libration points
 caused by the E-field is given in Fig. 2.

4 Libration points stability

To study the stability of the new equilibrium positions
 (L_{1+} , L_{1-} , L_{2+} , L_{2-} , L_{3+} , L_{3-}) caused by the E-field,
 we use a standard linearization procedure [12]. Firstly,
 the equations of relative motion are linearized in the
 small vicinity of the new equilibrium position. Then,
 the eigenvalues of the linearized plant matrix are
 determined. The conclusion about the equilibrium
 position stability is made on the basis of the real part of
 these eigenvalues. Let denote the position of the
 Lagrange point as (x_0, y_0) . The body M is located at the
 point with coordinates $(x_0 + \xi, y_0 + \eta)$. Calculating
 the body velocity components (ξ', η') , substituting
 these quantities into Eqs. (13), (14) and expanding
 result in a Taylor series gives

$$\xi'' - 2\eta' = \xi \frac{\partial^2 U}{\partial x^2} \Big|_0 + \eta \frac{\partial^2 U}{\partial x \partial y} \Big|_0 + \dots \tag{32}$$

$$\eta'' + 2\xi' = \xi \frac{\partial^2 U}{\partial x \partial y} \Big|_0 + \eta \frac{\partial^2 U}{\partial y^2} \Big|_0 + \dots \tag{33}$$

where the suffix zero means that after the partial If the
 displacements ξ and η are small, we may neglect terms
 involving squares, products and higher-degree terms
 in ξ and η , and so the equations become

$$\xi'' - 2\eta' = \xi U_{xx} + \eta U_{xy} \tag{34}$$

$$\eta'' + 2\xi' = \xi U_{yx} + \eta U_{yy} \tag{35}$$

where

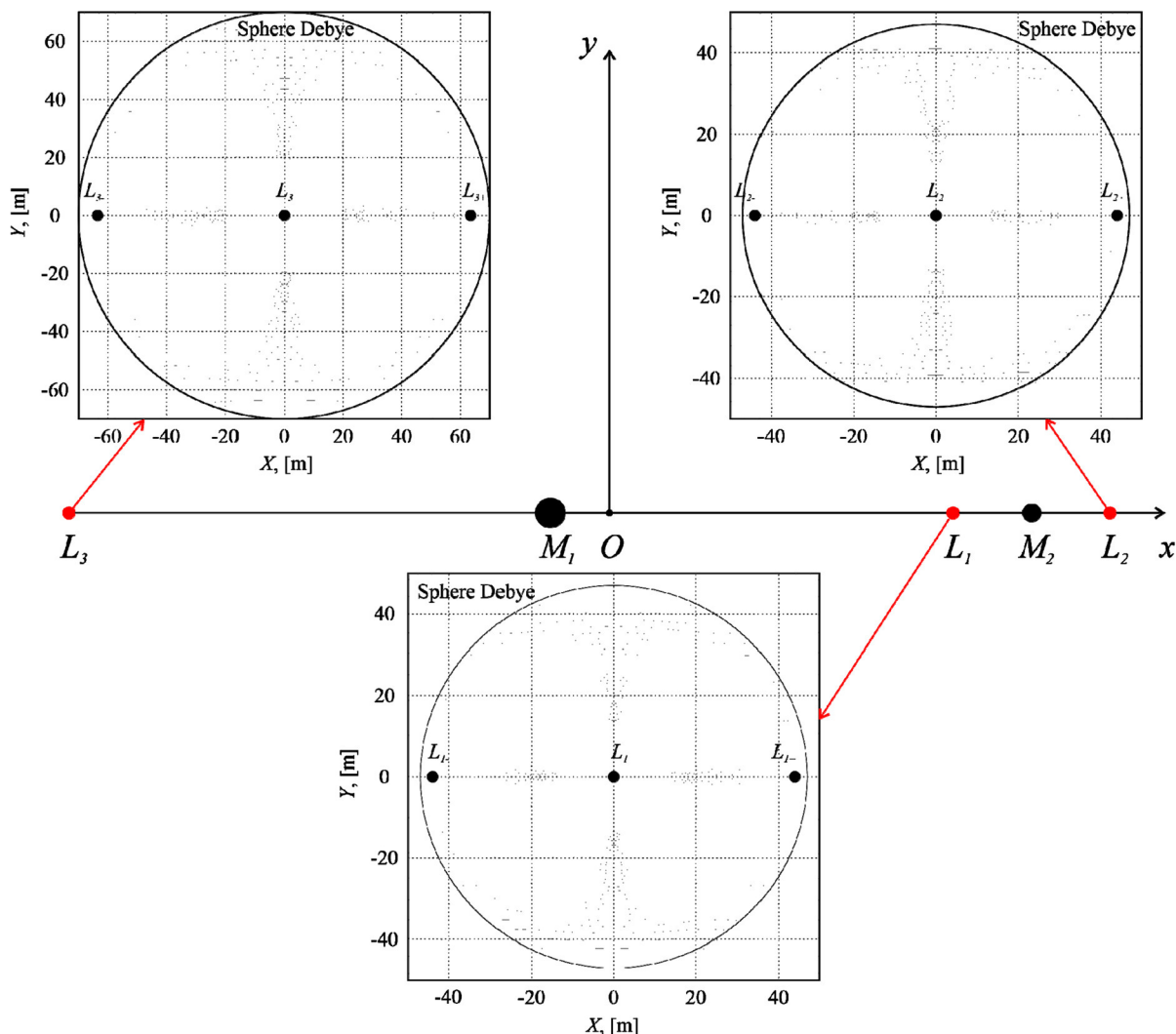


Fig. 2 Splitting the collinear libration points, when $\Phi = \frac{kcqoq}{md^3\omega^2} = -9 \cdot 10^{-16}$

$$\begin{aligned}
 U_{xx} &= \left. \frac{\partial^2 U}{\partial x^2} \right|_0, & U_{yy} &= \left. \frac{\partial^2 U}{\partial y^2} \right|_0, \\
 U_{xy} = U_{yx} &= \left. \frac{\partial^2 U}{\partial x \partial y} \right|_0 = \left. \frac{\partial^2 U}{\partial y \partial x} \right|_0
 \end{aligned}
 \tag{36}$$

341 and the U are constant since they are evaluated at the
 342 Lagrange point. These are linear differential equations
 343 with constant coefficients, the general solution of
 344 which may be written as

$$\xi = \sum_{i=1}^4 \alpha_i \exp(\lambda_i t), \quad \eta = \sum_{i=1}^4 \beta_i \exp(\lambda_i t)
 \tag{37}$$

346 where α_i are integration constants, the constants β_i

dependent upon α_i and the constants appearing in the
 347 differential equations. The λ_i are the roots of the
 348 characteristic determinant of Eqs. (34) and (35) set
 349 equal to zero and rewritten as
 350

$$\begin{vmatrix}
 \lambda^2 - U_{xx} & -2\lambda - U_{xy} \\
 2\lambda - U_{xy} & \lambda^2 - U_{yy}
 \end{vmatrix} = 0
 \tag{38}$$

or 352

$$\lambda^4 + (4 - U_{xx} - U_{yy})\lambda^2 + U_{xx}U_{yy} - U_{xy}^2 = 0
 \tag{39}$$

The solution is stable when all λ_i obtained from
 353 Eq. (39) are pure imaginary numbers. Since, along
 354 with any root λ , the biquadratic characteristic equation
 355 also has a root $-\lambda$, then the solution is unstable when
 356
 357

358 any of the λ_i are real or complex numbers with a
 359 nonzero real part. Now, defining the following quantities
 360 A, B, C, D and E as

$$A = \frac{1 - \mu}{\rho_1^3} + \frac{\mu}{\rho_2^3} \tag{40}$$

362 $B = 3\left(\frac{1 - \mu}{\rho_1^5} + \frac{\mu}{\rho_2^5}\right)$ (41)

364 $C = 3\left(\frac{1 - \mu}{\rho_1^5}(x_0 + \mu) + \frac{\mu}{\rho_2^5}(x_0 - (1 - \mu))\right)$ (42)

366 $D = k \frac{\Phi}{|\rho|^3}$ (43)

368 and

$$E = k \frac{\Phi}{|\rho|^5} \tag{44}$$

370 We find that

$$U_{xx} = 1 - A + 3(1 - \mu) \frac{(x_0 + \mu)^2}{\rho_1^5} + 3\mu \frac{(x_0 - (1 - \mu))^2}{\rho_2^5} + D - 3E(\alpha - x_0)^2 \tag{45}$$

372 $U_{yy} = 1 - A + By_0^2 + D - 3Ey_0^2$ (46)

374 $U_{xy} = Cy_0 + 3E(\alpha - x_0)y_0$ (47)

376 In the straight line solution, $y_0 = 0$, so that

$$\rho_i^2 = (x_0 - x_i)^2, \quad \rho^2 = (x_0 - \alpha)^2 \tag{48}$$

378 Hence

$$U_{xx} = 1 + 2A - 2D, \quad U_{yy} = 1 - A + D, \quad U_{xy} = 0 \tag{49}$$

380 Applying the values from (49) in Eq. (39) we obtain

$$\lambda^4 + (2 - A')\lambda^2 + (1 + A' - 2A^2) = 0 \tag{50}$$

382 where

$$A' = A - D = \frac{1 - \mu}{\rho_1^3} + \frac{\mu}{\rho_2^3} - k \frac{\Phi}{\rho^3} \tag{51}$$

384 It can be shown that

$$1 + A' - 2A^2 < 0 \tag{52}$$

for values of μ up to its limit of $\frac{1}{2}$. Hence, the four roots
 of equation (50) consist of two real roots, numerically
 equal but opposite in sign, and two conjugate pure
 imaginary roots. Hence the solution is unstable.
 Obviously, condition (52) with quadratic dependence
 on the left side is satisfied for any A' greater than unity

$$A' = A - D > 1 \tag{53}$$

Let us demonstrate that all the new equilibrium
 positions ($L_{1+}, L_{1-}, L_{2+}, L_{2-}, L_{3+}, L_{3-}$) satisfy this
 condition. Consider the first two of these points
 L_{1+}, L_{1-} located within the Debye sphere with respect
 to the point L_1 . Since these points are located between
 M_1 and M_2 , then $\rho_1, \rho_2 < 1$ and therefore

$$A = \frac{1 - \mu}{\rho_1^3} + \frac{\mu}{\rho_2^3} > 1 - \mu + \mu = 1 \tag{54}$$

Now consider the parameter D , which in conse-
 quence of (43) and (1) within the Debye sphere is
 always negative:

$$D = k \frac{\Phi}{|\rho|^3} < 0 \tag{55}$$

Thus, the condition (53) is satisfied for the equilib-
 rium positions L_{1+}, L_{1-} , and hence the condition (52)
 is also satisfied, hence the equilibrium positions
 L_{1+}, L_{1-} are unstable.

We now investigate the stability at the other
 collinear equilibrium positions L_{2+}, L_{2-}, L_{3+} and
 L_{3-} , found from the four equations (28)–(31). Below
 we prove that at these points $A' > 1$ as well. For this
 purpose equation (25) can be rewritten as

$$0 = x\left(1 - \frac{1 - \mu}{\rho_1^3} - \frac{\mu}{\rho_2^3}\right) + \frac{(1 - \mu)}{\rho_1^3}x_1 + \frac{\mu}{\rho_2^3}x_2 + k \frac{\Phi(x - \alpha)}{(x - \alpha)^3} \tag{56}$$

Considering that $x_1 = -\mu, x_2 = 1 - \mu$, get

$$x\left(\frac{1 - \mu}{\rho_1^3} + \frac{\mu}{\rho_2^3} - 1\right) = \mu(1 - \mu)\left(\frac{1}{\rho_2^3} - \frac{1}{\rho_1^3}\right) + k \frac{\Phi(x - \alpha)}{(x - \alpha)^3} \tag{57}$$

comparing this expression with Eqs. (40), (43) and
 (53) write it as

Author Proof

$$\begin{aligned}
 A' - 1 &= \frac{1 - \mu}{\rho_1^3} + \frac{\mu}{\rho_2^3} - 1 - k \frac{\Phi}{|\rho|^3} \\
 &= \frac{\mu(1 - \mu)}{x} \left(\frac{1}{\rho_2^3} - \frac{1}{\rho_1^3} \right) - k \frac{\Phi}{|\rho|^3} + k \frac{\Phi(x - \alpha)}{x(x - \alpha)^3}
 \end{aligned} \quad (58)$$

420 Note that at the points L_{2+} and L_{2-} , the conditions
 421 $x > 0$ and $\rho_2 < \rho_1$ are satisfied, and at the points L_{3+}
 422 and L_{3-} , the conditions $x < 0$ and $\rho_2 > \rho_1$. Besides

$$-k \frac{\Phi}{|\rho|^3} + k \frac{\Phi(x - \alpha)}{x(x - \alpha)^3} > 0 \quad (59)$$

424 since $\Phi < 0$ and x always many orders of magnitude
 425 greater than ρ , which does not exceed the relative
 426 Debye length (23). Therefore, in these considered
 427 cases we get

$$A' > 1 \quad (60)$$

429 It follows that condition (52) is also satisfied. Thus,
 430 we have proved that the all new collinear equilibrium
 431 points (L_{1+} , L_{1-} , L_{2+} , L_{2-} , L_{3+} , L_{3-}) are unstable.

432 5 Numerical simulation

433 This section shows the effect of the electrostatic
 434 charge level on the capture of the E-capsule in the
 435 vicinity of the Mars-Fobos libration point L_1 , in which
 436 the orbiter together with the E-capsule generates the
 437 attracting E-field. Note that the Debye length near the
 438 L_1 point is unknown; approximate Debye length
 439 values are given for the Stickney crater, located on
 440 Phobos' surface directly under the L_1 point. Depend-
 441 ing on Mars local time, this parameter ranges from 13
 442 to 47 m [14]. In the absence of accurate data, all
 443 calculations are performed for $\lambda_D = 45m$. Since we
 444 study the motion of the capsule relative to the orbiter,
 445 which is in the L_1 point, it makes sense to pass from the
 446 frame Oxy to the frame L_1XY (Fig. 3) by changing the
 447 variable

$$x = X + a_1, \quad y = Y \quad (61)$$

449 where a_1 is abscissa of the Mars-Phobos L_1 point

450 Then taking into account (61), the motion equations
 451 (7) and (8) can be rewritten as

$$\ddot{X} = \frac{\partial W_E}{\partial X} + \omega^2(X + a_1) + 2\omega\dot{Y} \quad (62)$$

$$\ddot{Y} = \frac{\partial W_E}{\partial Y} + \omega^2 Y - 2\omega\dot{X} \quad (63) \quad 453$$

where the effective potential is written as 455

$$\begin{aligned}
 W_E(X, Y) &= G \left(\frac{m_1}{\sqrt{(X + a_1 + d\mu)^2 + Y^2}} \right. \\
 &\quad \left. + \frac{m_2}{\sqrt{(X + a_1 - d(1 - \mu))^2 + Y^2}} \right) \\
 &\quad - k \frac{P}{m\sqrt{X^2 + Y^2}}
 \end{aligned} \quad (64)$$

where $P = k_C q_O q < 0$ is the charge level. 457

All trajectories of the capsule $m = 10 \text{ kg}$ begin with 458
 the same initial conditions in the vicinity of point L_1 459
 from the side of Phobos in the frame L_1XY 460

$$\begin{aligned}
 X_0 &= 81.533 \text{ m}, \quad Y_0 = 10.829 \text{ m}, \\
 \dot{X}_0 &= -0.043 \text{ m/s}, \quad \dot{Y}_0 = -0.017 \text{ m/s}
 \end{aligned} \quad (65)$$

Figure 3 demonstrates the E-capsule trajectories 462
 for different charge levels: 463

$$P = k_C q_O q = 0, \quad -0.28, \quad -0.32, \quad -0.40 \text{ [N} \cdot \text{m}^2]$$

In the first case the E-field is absent, therefore, the 465
 capsule does not reach the vicinity of the point L_1 , the 466
 same thing we can see when the charge level is not 467
 high enough ($P = -0.28 \text{ N} \cdot \text{m}^2$). If the charge level is 468
 equal $P = -0.32 \text{ N} \cdot \text{m}^2$ and more 469
 ($P = -0.40 \text{ N} \cdot \text{m}^2$), there are several turns of the 470
 capsule around the point L_1 , and the greater the charge 471
 level, the more turns the E-capsule performs around 472
 the point L_1 . 473

474 6 Conclusion

This paper shows within the framework of the planar 475
 circular restricted three-body problem that the artifi- 476
 cial attractive E-field at one of the collinear libration 477
 points causes the splitting of this point into two other 478
 unstable collinear libration points located within the 479
 Debye length. This fact was proved analytically, using 480

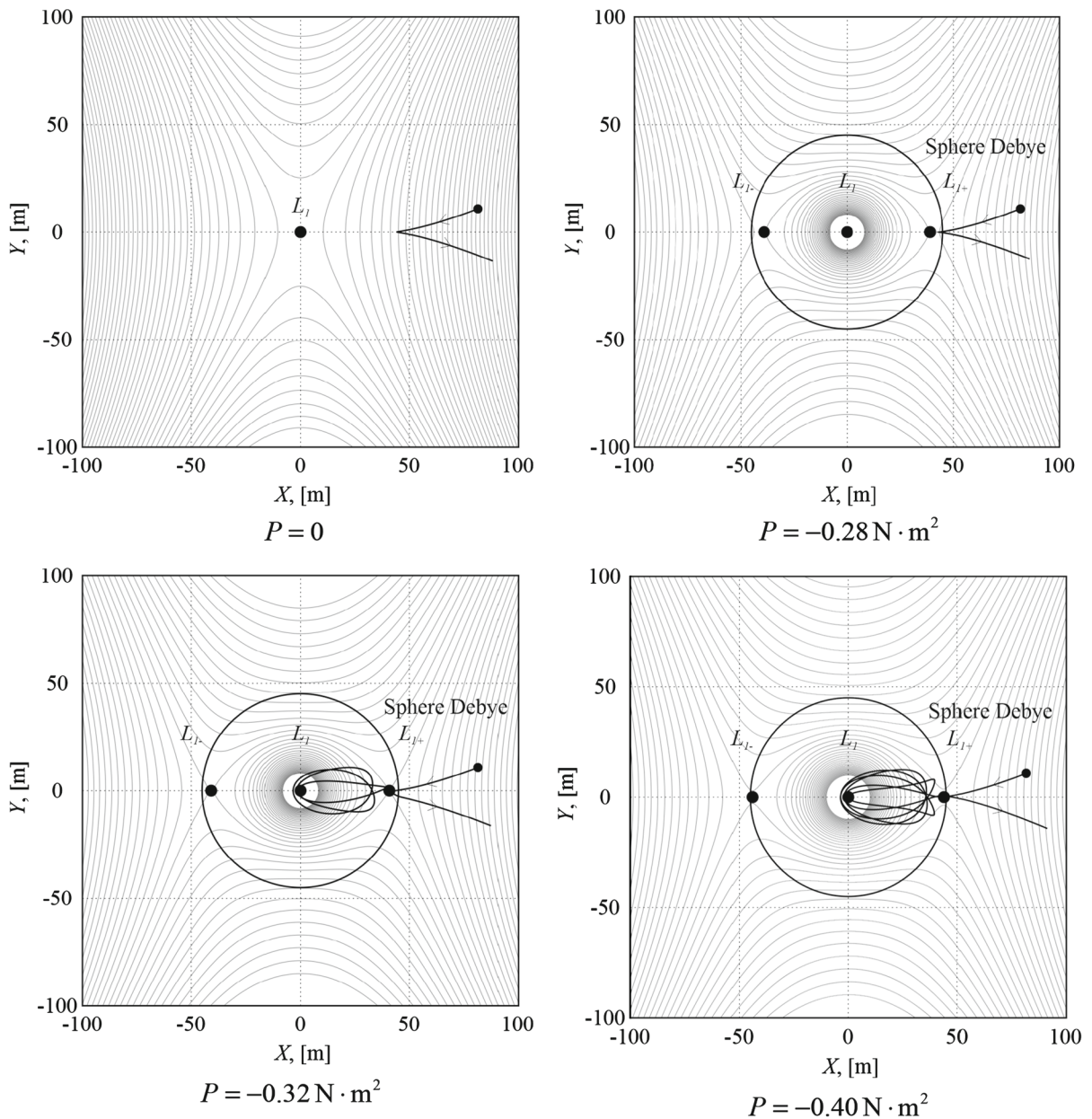


Fig. 3 The capsule trajectories and Contour plot of the effective potential $W_E(X, Y)$ in the frame L_1XY

481 the corresponding analytic equations, the new Jacobi
 482 integral, and confirmed by the numerical simulation.
 483 We have demonstrated the feasibility of the attracting
 484 mission the E-capsule in a small vicinity of the Mars-
 485 Fobos libration point L_1 .

486 **Acknowledgements** This study was supported by the Russian
 487 Science Foundation (Project No. 19-19-00085).
 488

Compliance with ethical standards 489

Conflict of interest The author declares that he has no conflict of interest. 490
 491

References 492

1. Szebehely, V.: The Restricted Problem of Three Bodies. Academic Press Inc., New York (1967) 493
 494

- 495
496
497
498
499
500
501
502
503
504
505
506
507
508
509
510
511
512
513
514
515
516
517
518
519
2. Connor Howell, K.: Three-dimensional, periodic, ‘halo’ orbits. *Celestial Mech.* **32**, 53–71 (1984). <https://doi.org/10.1007/BF01358403>
 3. Luo, T., Pucacco, G., Xu, M.: Lissajous and halo orbits in the restricted three-body problem by normalization method. *Nonlinear Dyn.* **101**, 2629–2644 (2020). <https://doi.org/10.1007/s11071-020-05875-1>
 4. Zotos, E.E.: Classifying orbits in the restricted three-body problem. *Nonlinear Dyn.* **82**, 1233–1250 (2015). <https://doi.org/10.1007/s11071-015-2229-4>
 5. Ferrari, F., Lavagna, M.: Periodic motion around libration points in the elliptic restricted three-body problem. *Nonlinear Dyn.* **93**, 453–462 (2018). <https://doi.org/10.1007/s11071-018-4203-4>
 6. Woo, P., Misra, A.K.: Equilibrium points in the full three-body problem. *Acta Astronaut.* **99**, 158–165 (2014). <https://doi.org/10.1016/j.actaastro.2014.02.019>
 7. Biggs, J.D., Negri, A.: Orbit-attitude control in a circular restricted three-body problem using distributed reflectivity devices. *J. Guid. Control Dyn.* **42**(12), 2712–2721 (2019). <https://doi.org/10.2514/1.G004493>
 8. Alessi, E.M., Sánchez, J.P.: Semi-analytical approach for distant encounters in the spatial circular restricted three-body problem. *J. Guid. Control Dyn.* **39**(2), 351–359 (2016). <https://doi.org/10.2514/1.G001237>
 9. Shibata, T., Bennett, T., Schaub, H.: Prospects of a hybrid magnetic/electrostatic sample container retriever. *J. Spacecraft Rockets* **57**(3), 434–445 (2020). <https://doi.org/10.2514/1.A34509>
 10. Dankanich, J., Klein, E.: Mars ascent vehicle development status, IEEE Aerospace Conference, Big Sky, USA (2012). <https://doi.org/10.1190/AERO.2012.6187295>
 11. Schaub, H., Junkins, J.: *Analytical Mechanics of Space Systems*, AIAA EducationSeries, 2nd edn. Reston, VA (2009)
 12. Roy, A.E.: *Orbital motion*. IoP, Bristol and Philadelphia (2005)
 13. Hartzell, C.M., Farrell, W., Marshall, J.: Shaking as means to detach adhered regolith for manned Phobos exploration. *Adv. Space Res.* **62**(8), 2213–2219 (2018). <https://doi.org/10.1016/j.asr.2017.09.010>
 14. Martynov, M.B., et al.: Planetary protection principles used for Phobos-Grunt mission. *Sol. Syst. Res.* **45–7**, 593–596 (2011). <https://doi.org/10.1134/S0038094611070185>

Publisher’s Note Springer Nature remains neutral with regard to jurisdictional claims in published maps and institutional affiliations.

520
521
522
523
524
525
526
527
528
529
530
531
532
533
534
535
536
537
538
539
540
541
542